Surface Discharges for High-Speed Boundary Layer Control

Roger L. Kimmel[*] and James R. Hayes.[†]
Air Force Research Laboratory, WPAFB, OH 45433

Jim W. Crafton[‡] and Sergey D. Fonov[§]
Innovative Scientific Solutions, Dayton, OH

and

James Menart[**] and Joseph Shang[††]
Department of Mechanical and Materials Engineering, Wright State University, OH, 45435

Surface plasma discharges have been shown to be effective in altering laminar boundary layers. Judicious choice of electrode shape can create a discharge that emulates a wedge or a bump. The "virtual wedge" discharge has been shown to create a local pressure rise with potential applications to vehicle control. The "virtual bump" creates a lesser pressure rise, but strong distortion of the boundary layer. In the current work the effect of the bump discharge on laminar shock boundary layer interactions is explored. Laminar shock boundary layer interactions are created with an impinging shock on a flat plate at a freestream Mach number of 5. The primary instrumentation is a low-modulus elastomer doped with a pressure-sensitive dye. Intensity distributions from the dye are imaged to interrogate the surface pressure. Displacement of surface markers provides surface shear information. Results show the presence of Görtler vortices in the reattaching shear flow. The Görtler vortices are also evident in temperature-sensitive paint images. These vortices are evident in the intensity images from the elastomer, which can be related to the surface pressure, but are not readily evident in the surface shear measurements. The DC discharge moves the separation line upstream, but does not change the wavelength of the Görtler vortices.

I. Introduction

Surface plasma discharges have been shown to be an effective means of controlling boundary layers. [1,2,3,4,56] High-frequency point and line discharges have been used to excite boundary layer instabilities. DC discharges have been used at higher energy levels to affect the mean boundary layer. Recent work at the Air Force Research Laboratory has shown that DC discharges can elevate pressures on a flat plate and significantly distort the boundary layer. Local heating of the boundary layer, primarily by the cathode, creates an expansion of the boundary layer fluid that deflects streamlines, thus modifying the flowfield. 2D discharges act as virtual wedges, creating a local pressure rise. Circular electrodes emulate a bump or weak jet, creating less pressure rise but with a vortex downstream.[7] Computations for a 2D discharge show that the skin friction is significantly altered near the discharge, with an initial dip in skin friction followed by a region of higher skin friction.[6]

This ability to manipulate skin friction and boundary layer profile indicates a possibility for modulating shock-boundary layer interaction. Separation could be either inhibited or promoted depending on the shape of the discharge and its location with respect to the separation. For example, Figure 1 from Ref. 6 shows the computed surface shear stress for an undisturbed, laminar flat plate boundary layer compared to the shear stress in the presence

[*] Senior Research Engineer, AFRL/VAAA, 2130 8th St, WPAFB, OH 45433 Associate Fellow AIAA.
[†] Senior Research Engineer, AFRL/VAAI, 2130 8th St, WPAFB, OH 45433.
[‡] Scientist, 2766 Indian Ripple Road, Dayton, OH 45440-3638
[§] Senior Scientist, 2766 Indian Ripple Road, Dayton, OH 45440-3638 sfonov@innssi.com, www.innssi.com/psp
[**] Associate Professor, Dept. of Mech. and Materials Eng., Wright State University, OH, 45435 Member AIAA
[††] Research Professor, Dept. of Mech. and Materials Eng., Wright State University, OH, 45435 Fellow, AIAA

of a 2D DC surface discharge of 19W/cm and a 2D heated strip with equivalent power input. The cathode is located near the upstream perturbation in shear stress, the anode near the downstream perturbation. Placement of a shock-boundary layer interaction near the dip in surface shear upstream of the cathode might be expected to promote separation. Conversely, placement of the interaction downstream of the cathode where shear stress rises above undisturbed flat plate values might inhibit separation.

The boundary layer distortion created by the circular electrodes might also provide a means of controlling shock boundary layer interactions. Spanwise Pitot pressure surveys downstream of a circular electrode discharge are shown in Figure 2. The electrode configuration is similar to that shown in the top of Figure 3. Surveys were conducted at three stations downstream of the electrodes at a constant height of 0.51 cm above the plate surface. The survey at 3.18 cm, immediately downstream of the cathode, is above the edge of the boundary layer and shows local increases in Pitot pressure to the left and right of the cathode. These are the result of a rounded bow shock created by the displacement of fluid about the cathode. Additional surveys shown in Ref. 7 demonstrate the three-dimensional nature of the shock structure from this discharge. The Pitot surveys show some left-right asymmetry, presumably due to a small amount of anode heating. Surveys farther downstream at 5.72 and 8.26 cm are within the growing boundary layer and show the development of a Pitot pressure deficit. This deficit is due to a local thickening of the boundary layer due to Joule heating of the fluid near the cathode. It was surmised that since the shock structure of the circular discharge is similar to that from a bump or weak jet, that a horseshoe vortex may be created, as is typical for a blunt solid obstruction. Some evidence for this structure may be seen at the most downstream station, but the Pitot pressure evidence is equivocal. Given the pronounced changes in Pitot pressure, however, coupled with insignificant changes in surface pressure, it was surmised in Ref. 7 that the circular electrode discharge created primarily a vertical disturbance. The utility of vortex generators in modifying shock boundary layer interactions is well-known. The circular electrode discharge may provide a means to create an on-demand, high-bandwidth vortex generator.

The aim of the current work is to explore the effect of the circular electrode discharges on laminar shock boundary layer interactions. As noted above, the most notable flow alteration created by the circular electrode discharges is a deficit in Pitot pressure. This might be expected to promote, rather than inhibit separation. Since this initial work is exploratory in nature, this is acceptable. The goal of the work is merely to determine if low-power discharges from circular electrodes create enough flow modification to change a separated flow. If the separation can be modified by the discharge, this opens the way to exploring more useful electrode configurations and placements.

II. Test Conditions and Experimental Configuration

Tests were conducted in the AFRL/VA plasma channel. The plasma channel is a small scale, low-density flow channel designed for the study of plasma dynamics and magneto-aerodynamic phenomena. It consists of a two-dimensional conical nozzle operating at a stagnation temperature of about 270K and a stagnation pressure range of 0.4 to 1.0 atmosphere. The current tests were carried out at stagnation pressures of 375-560 Torr, with stagnation temperatures of approximately 280K. The bulk of the measurements reported in this paper were carried out at 560 Torr stagnation pressure. Pitot probe measurements showed the freestream Mach number on the tunnel centerline to be 5.3 +/-3%. The nozzle exit dimensions are 178mm in height and 74mm in width. The entire channel is fabricated from acrylic plastic and assembled with nylon screws. A test cabin is provided to house a model support and instrumentation probes. The facility, including flow calibration, is described in more detail in a prior publication.[8]

The model in the current study consisted of a 5.1 cm wide wide by 10.2 cm long flat plate constructed of phenolic resin, with a circular cathode / anode pair (Figure 3). The cathode consists of a 1.59 cm diameter copper discs, and the anode of a 0.32 cm dia brass pin. The electrode edges were sealed with boron-nitride paint. The DC discharge is provided by a Universal Voltronics reversible polarity switching power units. Diagonal lines emanating from the upstream corners of the model in the diagram indicate Mach lines for Mach 5.0. These lines approximately delineate the 2D flow region in the middle of the model. The model bottom leading edge consists of a 20-degree ramp, so the disturbance propagating from the bottom to the top of the plate within the Mach cones is compressive.

A 1 mm deep pocket was milled behind the cathode to receive a shear-stress-sensitive film. The film is made of a flexible elastomer. The shear modulus of the film was adjusted to be in the range 100-500 Pa by modifying the material composition. Shear deformation of the film caused by the flow is measured by monitoring the displacement of markers applied to the film. The shear stress may be determined by using Hooke's law for shear strain.[9] Additional fiducial markers were fixed to the bottom of the pocket on the left side and rear of the pocket. These markers were used to compensate for any gross model displacements that occur during wind-on conditions.

Normal deformation of the film may be related mainly to the surface static pressure.[9,10] The normal deformation is measured by doping the elastomer with a dye. The intensity of the dye fluorescence is proportional to the film thickness due to low compressibility of the elastomer. A local increase in pressure, for example, thins the elastomer layer immediately beneath the normal load and causes it to bulge up around this region. In this paper intensity fields were obtained by normalizing wind-off by wind-on data, so the measured intensity is proportional to the film thickness.

A shock generator was placed above the flat plate model to create a shock-boundary layer interaction on the flat plate. A schematic of the shock generator and flat plate model are shown in the bottom of Figure 3. The shock generator was constructed of steel and was 3.8 cm wide in the spanwise dimension and 2.54 cm long in the streamwise dimension. The shock generator angle was adjustable from 0 to 10 deg. The leading edge of the shock generator was placed in either of two locations, 1.27 cm downstream of the test plate leading edge and 1.27 cm above it, or at the same x-location and 2.54 cm above the test plate.

III. Results

A. No Shock Generator Present

Initial measurements were conducted with no shock generator in the wind tunnel in order to obtain a baseline. Plasma-off and plasma-on surface displacement maps are presented in Figure 4 and Figure 5 respectively for a stagnation pressure of 375 Torr. The boundary layer is laminar for this condition. The plate was illuminated from the top, and viewed obliquely from the top left. The field of view for Figure 4 and Figure 5 is indicated by the shaded rectangle in Figure 6. Only the elastomer is visible in the image. The remainder of the imaged is coded as blue Flow is from left to right, and the cathode is immediately to the left of the elastomer in these images. In these figures the magnitude of the surface displacement in the plane of the flat plate, which approximates the surface shear stress, is color coded. Pseudo-limiting surface streamlines are obtained by tracing streamlines through the displacement vectors and are superimposed on the displacement magnitude contours. A zero pressure gradient flat plate boundary layer would have a shear on the order of 3 Pascal near the end of the plate, which is consistent with shear measured in this test. For the plasma-off case, the surface shear stress vectors near the edge of the plate turn inward, due to the local pressure field on the bottom of the plate that propagates around the edge. Between the Mach cones emanating from the corners of the plate, the flow is relatively two-dimensional.

The discharge-on case is shown in Figure 5. When the plasma is on, a portion of the elastomer directly behind the cathode is masked by the plasma glow, and is represented by the blue region. With a 50 mA discharge, shear stress vectors behind the cathode are directed inwards toward the centerline, indicating a crossflow component created by the plasma. The streamline convergence on the centerline strengthens in the downstream direction, consistent with the growing distortion of boundary layer Pitot pressure observed in spanwise surveys (Figure 2). It is posited that this growing inflow of streamlines and the associated Pitot distortion is the signature of a vortex growing downstream of the discharge. In both the plasma-off and plasma-on cases a convergence of streamlines occurs at the downstream edge of the elastomer film in the center. This is an artifact created by the fiducial marker beneath the film.

The baseline measurements in the absence of a shock generator indicate that the elastomer is capable of resolving shear stress on the order of a few Pascal. Pseudo streamlines near the center of the plate show the flow to be fairly two-dimensional. The convergence of streamlines on the plate centerline downstream of the cathode in the presence of a discharge is consistent with the formation of a vortex behind the cathode.

B. Effect of Discharge on Shock Boundary Layer Interaction

Plasma-off and plasma-on intensity maps and pseudo-streamlines obtained from the surface shear deformation field are presented in Figure 7 and Figure 9 respectively for a stagnation pressure of 560 Torr and a shock generator angle of 7 deg. The x and z locations of the shock generator leading edge were 1.27 and 1.27 cm. The plate was illuminated from the top left and viewed obliquely from the top left. The resulting image was deskewed using bilinear interpolation with the corners of the elastomer bed as control points.[11] A portion of the elastomer bed on the upper left was obscured by the shock generator. Only the elastomer is visible in the image.

It should be noted that the viscous interaction at this Mach number and pressure is quite pronounced, so that the actual flow deflection due to the shock generator is larger than the actual generator geometrical deflection. The inviscid shock location is indicated by a yellow line on the figures. It is determined by calculating where a shock at Mach 5.2 from a wedge would intersect the plate surface. This is for reference only. The most notable feature in the intensity map is the presence of spanwise periodic intensity variations. The presence of these intensity variations suggests the presence of Görtler vortices associated with the reattachment. The Görtler instability, as shown

schematically in Figure 10, consists of counter-rotating vortices created by curvature of the flow.[12] Görtler vortices have previously been observed experimentally[13] and computationally[14] in hypersonic impinging shock interactions. To rule out the possibility that these structures were not inherent in the flow but an artifact of mechanical instabilities in the elastomer, tests were carried out using temperature sensitive paint on a solid model. Results are shown in Figure 11. Although the image is of poor quality due to the presence of inactive round electrodes beneath a layer of polyimide tape, these results also showed a spanwise periodicity, thus indicating that the vortices were a feature inherent in the flow and not due to instabilities in the elastomer layer.

Another indicator of Görtler vortices comes from the glow from the discharge. The discharge creates a purplish glow around the electrodes from excited nitrogen, but a green glow, presumably from copper ions emitted by the electrodes, is also created and is highly persistent downstream of the electrodes. Figure 12 compares the intensity field from the elastomer to the glow from the discharge. It is apparent that the glow also picks up a spanwise periodicity downstream of the attachment, and that the peaks in the plasma glow correlate with peaks in the elastomer fluorescence intensity, which in turn correlates with regions of higher surface pressure. Numerous factors may contribute to the modulation of the plasma intensity such as the temperature and density of the gas. Nevertheless, the surface intensity variations appear correlated with the boundary layer flow structure above them. The observation of bright, long-lived emission from the copper raises the possibility of using this glow in its own right as a flow visualization device. The use of glow discharges to visualize the flow in low-density hypersonic flows is not new.[15,16] However, in previous incarnations of this method only the excited gas molecules have been utilized for visualization. The persistent afterglow from the copper offers new potential for flow visualization

Spanwise Fourier transforms of the intensity distribution for 0 and 25 mA are shown in Figure 13. The Fourier transforms were obtained by taking the FFT on 64 points on spanwise lines. The magnitude of the resulting power spectrum was normalized by the broadband mean square of the data. The results in Figure 13 were obtained by averaging 24 lines of data where the periodicity in the image was most prominent. The minimum wavenumber resolution for each figure is slightly different due to different magnifications. The peak in the spectrum occurs at about 2-2.2 mm^{-1}, or at a wavelength of 2.9-3.1 mm. The discharge has virtually no effect on the predominant Görtler wavenumber. It should be noted that spanwise non-uniformities that act as excitation for the Görtler instability are presumably broadband, but the Görtler instability will selectively amplify only a narrow band. Although the normalized peak at the Görtler wavenumber in the presence of the 25 mA discharge is less than for the 0 mA discharge, absolute magnitudes cannot be compared between the two cases, due to contamination of the elastomer fluorescence from the discharge glow. However, it should be noted that the relative shapes of the spectra are different. The plasma-on case displays a relatively higher amplitude at low wavenumber compared to the no-discharge case. This indicates that in the presence of the discharge energy tends to redistribute from the Görtler wavenumber to lower wavenumbers.

Pseudo-streamlines in Figure 7 and Figure 9 show a separation line as evidenced by a convergence of limiting streamlines, with a region of reversed flow downstream. An attachment line from which streamlines diverge is evident downstream of this. The attachment line is associated with the highest intensity peaks from the Görtler instabilities. Interestingly, the spanwise periodicity occurs both upstream and downstream of reattachment. Higher-intensity lobes fall at the spanwise extremities of the attachment. These appear to be correlated with foci in the streamlines. As expected, the 25 mA discharge moves the separation line upstream. This upstream movement is probably due to the momentum deficit in the boundary layer created by the discharge.

It should be noted that although the Görtler vortices are quite evident in the elastomer fluorescence, there is no indication of them in the surface streamlines. It was hoped that periodic spanwise flow would be evident in the streamlines, but this is not the case. This is further reinforced by the Fourier transform of the spanwise component of surface in-plane displacement shown in Figure 1. This is somewhat reminiscent of oil flow observations (Refs. 13 and 14) in which the oil-flow accumulation was observed, but no finer detail of spanwise periodic streamlines were obtained. The authors speculate that perhaps the circulation associated with the Görtler vortex is low, such that spanwise flows were not resolvable with the current instrumentation. Magnified images also failed to resolve any such periodicity in the in-plane displacement.

IV. Conclusions and Future Work

Prior work has shown that surface plasma discharges are capable of altering laminar boundary layer profiles and surface shear stress. In the current work a shear stress sensitive elastomer was employed to examine the effects of the discharge from a circular electrode on a laminar shock boundary layer interaction. Results show that the shear-stress-sensitive elastomer method is useful for at least qualitative measurement of the shear stress field under low shear conditions. The impinging shock from a 7-deg deflection plate was sufficient to separate the boundary layer.

The intensity of the fluorescent dye in the elastomer, which may be related to the surface pressure, displayed a spanwise periodicity near the boundary layer reattachment. This periodicity is consistent with a Görtler instability, which has been observed by other investigators in similar shock boundary layer interactions. Similar periodicity was also observed in temperature sensitive paint on a solid-surface model and in the afterglow from copper ions convected downstream of the cathode, ruling out the possibility that the periodicity observed in the elastomer was due to aeroelastic effects. Although this spanwise periodicity was apparent both in the fluorescence intensity of the elastomer and the temperature-sensitive paint, no similar periodicity was observed in the limiting pseudo-streamlines obtained from the in-plane displacement of the elastomer. The authors speculate that the cross-flow component is too small to resolve with the current instrumentation.

The presence of a 25 mA discharge upstream of the interaction distorted the spanwise wavenumber spectrum of the intensity, transferring energy to lower wavenumbers, but did not change the dominant Görtler wavenumber. The discharge also caused the separation line to move upstream. This was anticipated based on the previously observed thickening of the boundary layer due to the discharge.

The observations from this preliminary experiment open numerous avenues for future research. These include the development and refinement of the elastomer film technique, development of copper ion glow as a flow visualization device, further investigation of Görtler vortices in these interactions, and development of shock boundary layer interaction control methods using surface discharges. Most notably, the interaction should be probed to fully map out the three-dimensional interaction, and the elastomer film technique should be calibrated to place it on a quantitative basis. The control method may be refined manipulating the electrode shape to create a stronger vortex and by operating it harmonically in order to couple into traveling instabilities in the boundary layer.

Acknowledgments

This work was sponsored by the Air Force Office of Scientific Research, monitored by Dr. John Schmisseur. The authors wish to acknowledge the contributions of AFRL/VAAI and Wyle Laboratories to wind tunnel operations, and ISSI to diagnostics. This paper is dedicated to the memory of Seymour Bogdonoff.

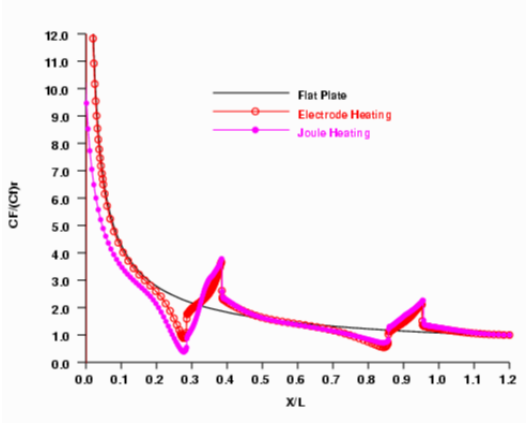

Figure 1 Computed surface shear stress distribution in 2D discharge in laminar boundary layer (Ref. 6).

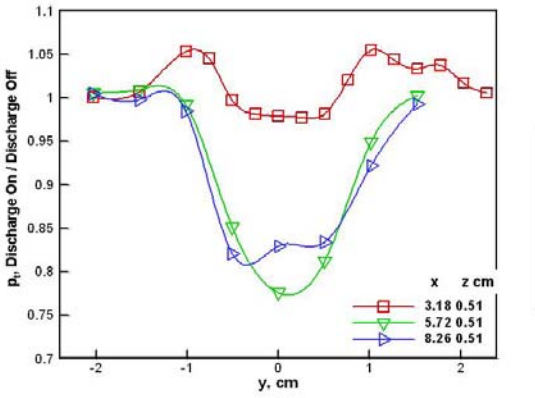

Figure 2 Spanwise Pitot pressure surveys downstream of circular electrode discharge at constant height above plate surface, 25 mA discharge.

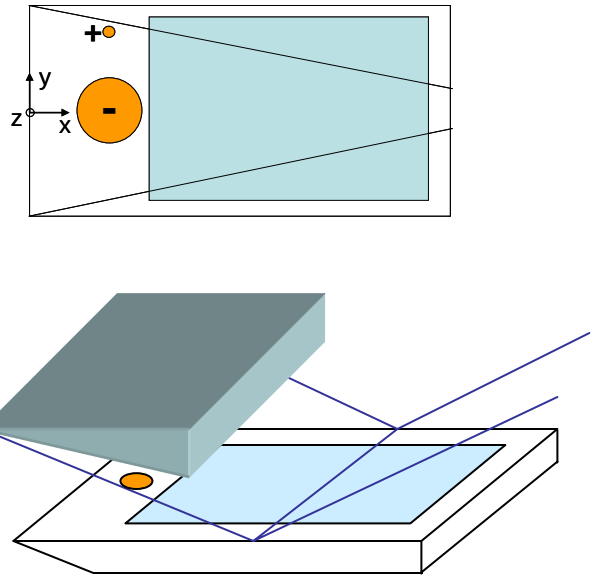

Figure 3 Schematic of flat plate and shock generator. Flow is from left-to-right.

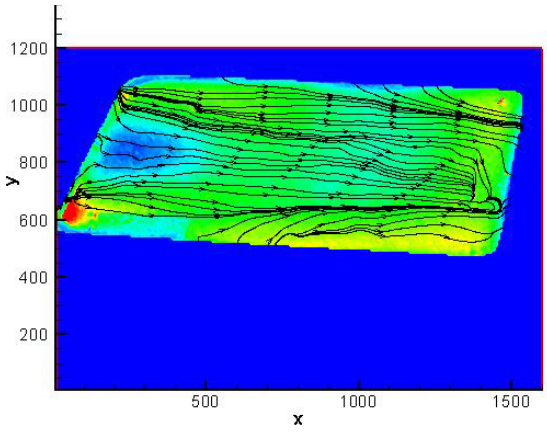

Figure 4 In-plane deflection field and limiting streamlines imaged with the shear-stress-sensitive elastomer in the absence of a shock-boundary layer interaction. Plasma-off, p0 = 375 Torr.

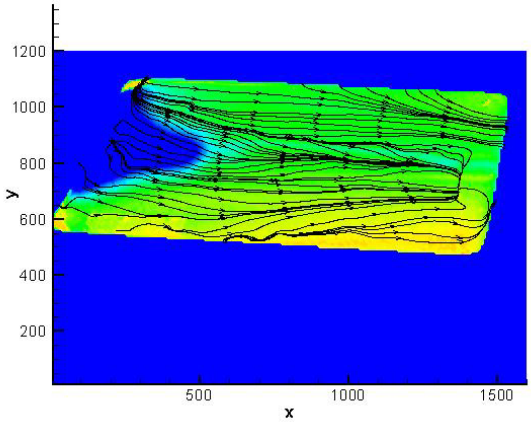

Figure 5 In-plane deflection field and limiting streamlines imaged with the shear-stress-sensitive elastomer in the absence of a shock boundary layer interaction. Plasma-on, p0 = 375 Torr.

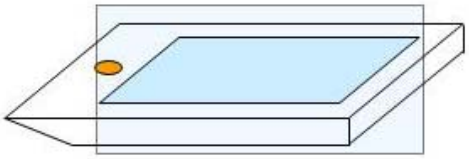

Figure 6 Field of view (shaded rectangle) shown in Figure 4 and Figure 5.

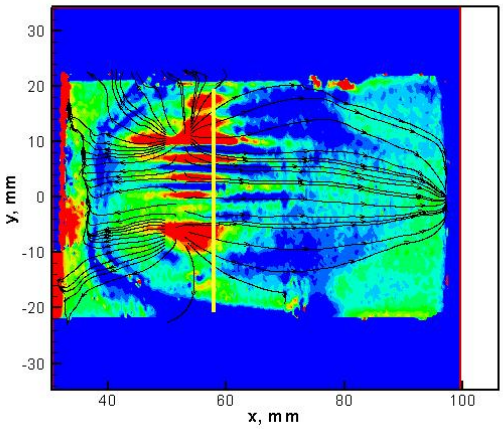

Figure 7 Intensity field and limiting streamlines imaged with the shear-stress-sensitive elastomer. Plasma-off, p0 = 560 Torr, shock generator at 7 deg. Flow left to right. Yellow line indicates inviscid shock location.

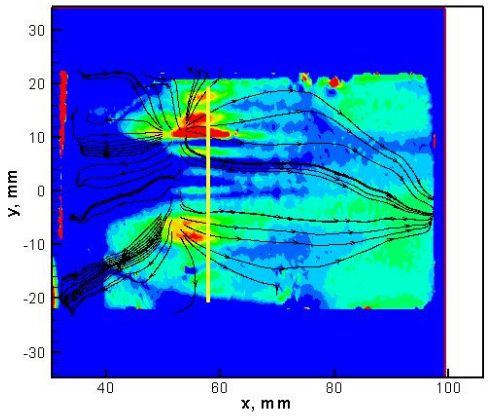

Figure 8

Figure 9 Intensity field and limiting streamlines imaged with the shear-stress-sensitive elastomer. 25 mA discharge, p0 = 560 Torr, shock generator at 7 deg. Flow left to right.

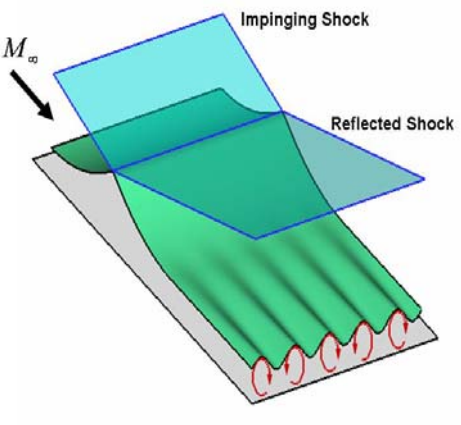

Figure 10 Schematic of Görtler vortices arising from impinging shock interaction.

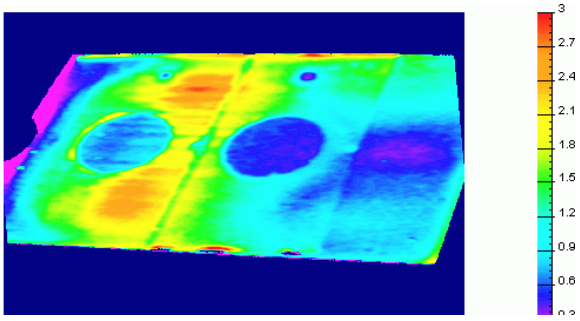

Figure 11 Temperature-sensitive paint imaging of impinging shock interaction. Plasma-off, p0 = 560 Torr, shock generator at 10 deg. Flow left to right.

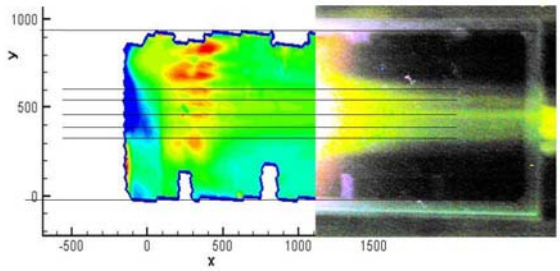

Figure 12 Comparison of elastomer intensity field to copper-ion glow from discharge, 25 mA discharge, p0 = 560 Torr, shock generator at 7 deg. Top view of model, flow from left to right.

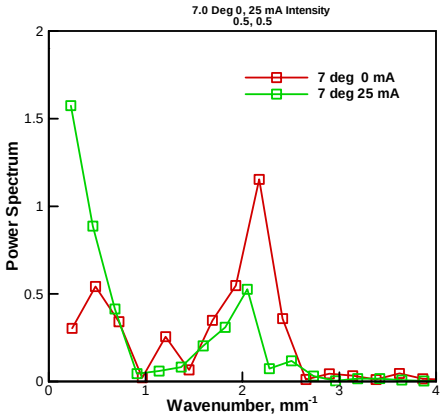

Figure 13 Fourier transform of spanwise intensity distribution for 7 deg shock boundary layer interaction, power-off and 25 mA discharge.

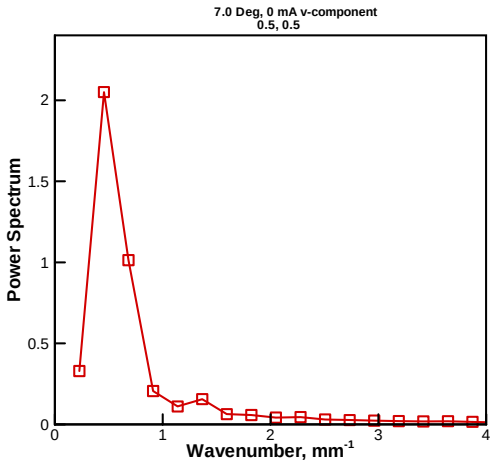

Figure 14 Spanwise Fourier transform of v (spanwise) surface displacement.

References

[1] Leonov, S., Bityurin, V., Savischenko, N., Yuriev, A., and Gromov, V., "Influence of Surface Electric Discharge on Friction of Plate in Subsonic and Transonic Airflow," AIAA paper 2001-0640, January 2001.
[2] Leonov, S., Bityurin, V., Klimov, A., Kolesnichenko, Y., and Yuriev, A., "Influence of Structural Electric Discharges on Parameters of Streamlined Bodies in Airflow," AIAA paper 2001-3057, June 2001.
[3] Leonov, S., Bityurin, V., Savelkin, K., and Yarantsev, D., "Effect of Electrical Discharge on Separation Processes and Shocks Position in Supersonic Airflow," AIAA paper 2002-0355, January 2002.
[4] Leonov, S., Bityurin, V., Savelkin, K., and Yarantsev, D., "Progress in Investigation for Plasma Control of Duct-Driven Flows," AIAA paper 2003-0699, January 2003.
[5] Leonov, S., Bityurin, V., and Yarantsev, D., "The Effect of Plasma Induced Separation," AIAA paper 2003-3853, June 2003.
[6] Shang, J.S., Surzhikov, S.T., Kimmel, R., Gaitonde, D., Menart, J., and Hayes J., "Plasma Actuators for Hypersonic Flow Control," AIAA paper 2005-0562, January 2005.

[7] Kimmel, R. L., Hayes, J. R., Menart, J. A., Shang, J. "Application of Plasma Discharge Arrays to High-Speed Flow Control," AIAA 2005-0946, January 2005.
[8] Shang, J. S., Kimmel, R., Hayes, J., and Tyler, C., "Performance of a Low-Density Hypersonic Magneto-Aerodynamic Facility," AIAA paper 03-0329, January 2003.
[9] Fonov, Sergey D., Goss, Larry P., Jones, E. Grant, Crafton, Jim W., Fonov, Vladimir S. and Ol, Michael, "New Method for Surface pressure Measurements," AIAA paper 2005-1029, January 2005.
[10] Fonov, Sergey D., Goss, Larry P., Jones, E. Grant, Crafton, Jim W., Fonov, Vladimir S. and Ol, Michael, "Surface Pressure and Shear Force Fields Measurements Using Elastic Polymeric Film," 11th International Symposium on Flow Visualization, August 9-12, 2004, University of Notre Dame, Notre Dame, Indiana,
[11] Castleman, K. R., *Digital Image Processing*, Prentice-Hall, Englewood Cliffs, NJ, 1979, pp. 113-119.

[12] Schlichting, H., *Boundary-Layer Theory*, 7th Edition, McGraw-Hill Book Company, New York, 1979, p 526.
[13] Henckels, A., Kreins, A. F., and Maurer, F., "Experimental investigations of hypersonic shock-boundary layer interaction," *Zeitschrift für Flugwissenschaften und Weltraumforuschung*, vol. 17, no. 2, pp. 116-124, Apr. 1993.
[14] Domröse, U., Krause, E., and Meinke, M., "Numerical simulation of laminar hypersonic shock-boundary layer interaction," *Zeitschrift für Flugwissenschaften und Weltraumforuschung*, vol. 20, no. 2, pp. 89-94. Apr. 1996.
[15] Nishio, M., "New Method for Visualizing Three-Dimensional Shock Shapes Around Hypersonic Vehicles Using an Electrical Discharge," *AIAA Journal*, vol. 28, no. 12, December 1990, pp. 2085-2091.

[16] Nishio, M., "Methods for Visualizing Hypersonic Shock-Wave / Boundary-Layer Interaction Using Electrical Discharges," *AIAA Journal*, vol. 34, no. 7, July 1996, pp. 1464-1467.